International Journal of
Nanomaterials and Nanostructures

ISSN: 2455-5584
Volume 10, Issue 2, 2024
July–December
DOI (Journal): 10.37628/IJNN

https://journalspub.com/journal/ijnn

Research IJNN

Mechanical, Thermal, and Electrical Properties of Poly(ether-ester)-Based Thermoplastic Elastomer Composites Filled with ZnO Nanoparticles

Haydar U. Zaman*

Abstract

A highly helpful technique to create novel polymeric materials with ordered and customized features is blending two or more immiscible polymers. The outstanding balance between processability and physical characteristics of thermoplastic polyester elastomers, particularly when using hydrogenated styrene–butadiene copolymer, makes them appealing materials for a variety of applications, including the automotive industry. New opportunities for tailored flexible composites with improved mechanical and chemical properties are made possible by reinforced polymers with zinc oxide. In this work, nano-zinc oxide particles were added to thermoplastic polyester elastomer via direct melt mixing, enhancing its mechanical, thermal, and electrical properties. Thermoplastic polyester elastomer had a particle content ranging from 1 to 5 weight percent. Before melting, zinc oxide nanoparticles were coated with maleated styrene ethylene butylene styrene to improve fine dispersion and surface adherence. We investigate the impact of polymer blends on the mechanical, thermal, and electrical characteristics of blends of thermoplastic polyester elastomers, both in the presence and absence of nanoparticles. The tensile test was used to determine how the concentration of nano-zinc oxide particles affected the yield strength, tensile strength, tensile modulus, and elongation at break. Except for elongation at break, all tensile parameters were enhanced by the nano-zinc oxide particles' stiff structure. Because of the establishment of chemical bonds, SEM studies reveal substantial interfacial contacts between the thermoplastic polyester elastomer matrix and nano-zinc oxide particles. The overall thermal characteristics of soft and hard parts, the melting temperature, and the thermal stability of nanocomposites are all improved by the inclusion of nano-zinc oxide particles. The mechanical, thermal stability, and electrical properties of a nanocomposite are all improved by adding more nanoparticles.

Keywords: Thermoplastic polyester elastomer, nano-ZnO, nanocomposites, mechanical, thermal, and electrical properties

***Author for Correspondence**
Haydar U. Zaman
E-mail: haydarzaman07@gmail.com

Assistant Professor, Department of Physics, National University of Bangladesh and Institute of Radiation and Polymer Technology, Bangladesh Atomic Energy Commission, Savar, Dhaka, Bangladesh

Received Date: September 29, 2024
Accepted Date: October 07, 2024
Published Date: October 14, 2024

Citation: Haydar U. Zaman. Mechanical, Thermal, and Electrical Properties of Poly(ether-ester)-Based Thermoplastic Elastomer Composites Filled with ZnO Nanoparticles. International Journal of Nanomaterials and Nanostructures. 2024; 10(2): 33–42p.

INTRODUCTION

The mechanical, thermal stability, and thermoplastic elastomers (TEs), which bridge the gap between rubber and plastic, are becoming more and more significant as creative materials. With their exceptional mechanical, thermal, and elasticity properties, TEs are made of a thermoplastic polyester elastomer (TPE) with a hard section made of poly(butylene terephthalate) (PBT) and a soft section made of poly(tetramethylene ether glycol terephthalate) [1]. The mechanical, thermal stability, and TEs are materials that exhibit special processing, strength, and flexibility because of the distinct

microstructures in each phase. The solid phase of elastomers melts and evaporates when they are processed at high temperatures. The hard and soft components form in a homogenous composite stage during the molten state. The type and quantity of the copolymer's hardening phase determines the characteristics of TE. The mechanical, thermal stability, and owing to its excellent processing and flexibility, TE is extensively utilized in a variety of industries, including sports, electrical equipment, and the automobile industry [2]. The mechanical, thermal stability, and various TEs, including styrene, urethane, amide, olefin, and ester, have been made available for commerce thus far, with uses in both home and automobile appliances [3–6]. The mechanical, thermal stability, and TPEs provide exceptional mechanical and thermal performance, among additional features [7]. Du Pont has successfully developed a family of cutting-edge segmented TPE under the brand name Hytrel®. TPE is a kind of thermoplastic that is categorized as a soft section made up of polyteramethylene glycol (PTMG) and is composed of a solid portion of the block structure PBT. Figure 1 shows the chemical makeup of PBT-block-poly(tetramethylene glycol) (PBT-PTMG)-based TPE.

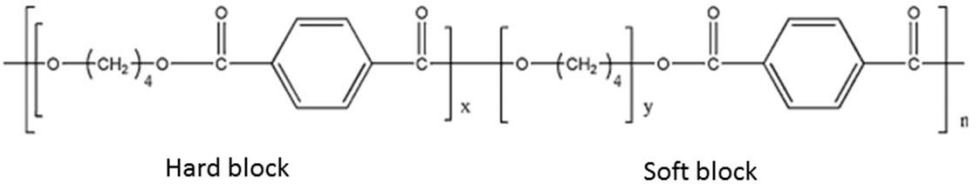

Figure 1. The TPE and its chemical composition.

TPE is widely used in automotive parts, such as hoses, gears, tubing, and gears, as well as electronics and electronic parts. It is also gradually replacing cross-linked rubbers due to its important processability and elasticity, superior oil and chemical resistance, superior lightweight, fatigue resistance, recyclability, and excellent heat resistance performance [8]. Compared to ordinary thermoplastic, TE exhibits elastomeric properties at room temperature and can evaporate at higher temperatures. Polystyrene (PS) and poly(vinyl methyl ether, PVME) are miscible in binary combinations, and several theories have been put out regarding how they interact. The ether group and aromatic ring of PS interact, according to Ryou et al.'s research [9], which was based on a change in the IR spectra of the miscible and immiscible PS/PVME film.

The characteristics of the polymer matrix can be greatly impacted by the aggregation of inorganic nanoparticles within it [10]. Acquiring composites could have many different mechanical, electrical, or thermal characteristics. These hybrid materials are composed of polymers that exhibit high carrier mobility, bandgap tenability, and structural flexibility, all of which have overlapping impacts on their special characteristics. As a result, they can enable a flexible design of their chemical and physical characteristics, satisfying the requirements of applications for end users [11]. The incorporated nanoparticles' form, size, and kind, as well as their interactions with the polymer matrix, determine the characteristics of polymer nanocomposites [12]. The impedance to particle agglomeration is crucial to the technology of polymer nanocomposite materials. For use in nanocomposite applications, several nanoparticles have been incorporated into the polymer matrix. Inorganic nano-metal oxide (nZnO) is used in the treatment of diabetes, wound healing, antibacterial, drug delivery, anti-cancer, anti-inflammatory, and high biomechanics. Its stability, large electronic machine coupling coefficient, high-catalytic activity, and high-illuminated transmittance, intense absorption of UV and infrared light, and high biomechanics are some of its other benefits [13–15]. Due to their tiny size, broad specific fields, and quantum effects on both organic and inorganic nanoparticles, ZnO nanoparticles can play a significant role in the development of mechanical and optical properties in polymers.

TPE/nZnO nanocomposites' enhanced mechanical strength, superior chemical, electrical, and optical capabilities, as well as their flexible design, have sparked a lot of research interest. Particles can indicate a decline in toughness because of their hardness, even when their mechanical characteristics have increased significantly. Therefore, adding both the elastomeric phase and the

inorganic reinforcement to the polymer matrix can result in an outstanding stiffness to toughness balance. To improve the toughness of hybrid composites, the most commonly used elastomers are styrene-ethylene-butylene-styrene (SEBS) [16], ethylene–propylene–diene monomer (EPDM) [17], and ethylene–propylene rubber (EPR) [18]. A challenge that may arise when investigating nanoparticles is the aggregation of particles. The aristocracy of the composite is decreased by agglomerates in the matrix; hence, dispersants and compatibilizers are needed to address this issue. In hybrid composites, maleated polypropylene (PPMA) or SEBS grafted maleic anhydride (SEBS-g-MA) is frequently utilized. In PP/montmorillonite nanocomposites, Tjong et al. [16] employed SEBS-g-MA. Maleic anhydride functioned as a compatibilizer between the inorganic particles and the matrix, while SEBS enhanced the composite's toughness. Numerous studies have used PP composites to examine the mechanical and physical characteristics of ZnO [19, 20]. The agglomeration of nano-ZnO particles and particle contents in the study presented here affect the mechanical, thermal, and electrical properties of TPEs.

EXPERIMENTAL

Materials

The polymer matrix TPE granules, grade Hytrel 6356, were kindly provided by M/S Rupal Plastics Ltd, Mumbai, India. The weight percentage and molecular weight of the PTMG part in this PBT–PTMG copolymer are approximately 50% and 100 g/mole, respectively. The average size of the nano-ZnO particles used in this study was 20 nm, and they were purchased from Changtai New Material Co., Ltd., China. The compatibilizer used in this study was approximately 10% SEBSMA (Kraton FG-1901X), with 1.84 wt% MA graft ratio and MFI of 20 dg/min (270°C/5kg), which was obtained from Shell Chemical Co (Houston, TX).

Methods

ZnO Nanoparticle Modification Using Compatibilizer

The nZnO particles were dried in a vacuum oven prior to modification. Toluene was dissolved in room temperature for 48 hours to employ SEBSMA. Further, this solution is gradually infused with pure nZnO particles, which are then combined for two hours using a mechanical mixer (IKA RW 20 digital). After eight hours of drying at 50°C, the mixture was pulverized. Five percent of the nZnO particle was made up of SEBSMA.

Preparing Nanocomposite

Prior to compounding, every component was dried for 48 hours at 60°C in a vacuum oven, and it was thereafter chilled to room temperature for usage. Before mixing, every ingredient was added right away to the extruder. 1, 3, and 5 wt% of nZnO were added to a Berstorff twin-screw extruder (ZE-25A UTX, KraussMaffei Berstorff GmbH, Germany) to extrude a TPE. TPE/1nZnO, TPE/3nZnO, and TPE/5nZnO were the codes assigned to the nanocomposites. The screws had a 25 mm diameter and a 44 length to diameter ratio (L/D). Processing temperatures varied from 200°C in the adjacent hopper to 220°C in the die, with a screw speed of 150 revolutions per minute. After cooling, the extruded product was crushed into tiny pellets. The resulting pellets were heated electrically and utilized to create thin plates in the hydraulic press. The pellets were preheated for five minutes, hot-pressed for a further five minutes at 210°C, and then cooled with water at a rate of 10°C per minute to room temperature.

Characterizations

Surface Topography and Particle Dispersion

The dispersion of nanoparticles and fracture surfaces were examined using SEM. Utilizing a SEM, JSM-6360LV from JEOL, Tokyo, Japan, the fracture surfaces of nanocomposites were examined. Prior to imaging, the samples underwent gold coating.

Differential Scanning Calorimetry

Differential scanning calorimetry (DSC, Perkin Elmer DSC-7) was used to examine the crystallization, melting behaviors, and crystalline enthalpy of nanocomposites in the N_2 atmosphere.

To verify a duplicate thermal history, each sample (5–8 mg) was heated from 30 to 280°C at a heating rate of 10°C/min. The sample was then maintained at 280°C. At a rate of 10°C per minute, the sample was cooled to 30°C.

Thermogravimetric Analysis

A thermogravimetric analyzer (TGA, TA Instruments Q500) was used to measure the thermal stability of the nanocomposites at a heating rate of 20°C/min in a N_2 environment.

Evaluation of Mechanical Properties

The Shimadzu Universal Testing Machine (type AG-1, Japan) was used to measure the tensile test. The samples measured 50 mm in gauge length, 10 mm in width, and 2 mm in thickness. The elongation at break, yield strength, tensile strength, and tensile modulus were all measured using a crosshead speed of 10 mm/min. Five repeat tests were carried out in order to establish an average value for each sample, and all experiments were carried out in accordance with ASTM-D 638-14 standard [21].

Electrical Tests

To manufacture tablets, uncoated and coated nanocomposites were finely chopped and subsequently pulverized. The dielectric characteristics have been measured with this tablet. The dielectric characteristics are measured at 10 kHz using a Marconi Universal Bridge (TF 1313 A). The bridge approach, which is a two-electrode method, was utilized to test the resistivity and dielectric constant of nanocomposites at a frequency of 10 kHz. Resistivity was measured using an electrometer (model-617).

RESULTS AND DISCUSSION

Nano-ZnO Particle Dispersion in TPE Matrix

It is commonly recognized that the mechanical properties of nanocomposites can be significantly impacted by the filler's dispersion inside the polymer matrix. A thermoplastic inorganic filler's dispersion is a difficult process. Since nanoparticles have a high propensity to aggregate, the issue is made worse when they are utilized as a filler. The TPE/3 wt% uncoated nZnO (3UnZnO), TPE/3 wt% coated nZnO (3CnZnO), and TPE/5 wt% coated nZnO (5CnZnO) nanocomposites are shown in TEM photomicrographs in Figure 2(a–c), respectively. ZnO nanoparticles are shown as dark areas in the TEM picture. The majority of the nZnO particles in the TPE/3CnZnO nanocomposite are uniformly distributed, as seen in the TEM image (Figure 2(b)). Most nanoparticles are smaller than 100 nm, with the smallest being less than 5 nm, according to TEM photomicrographs.

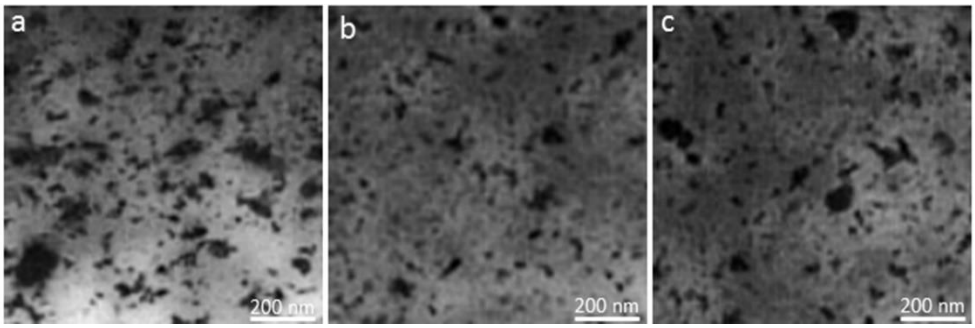

Figure 2. TPE/nZnO nanocomposites (w/w%) using TEM photomicrographs: (a) TPE/U3nZnO, (b) TPE/C3nZnO, and (c) TPE/C5nZnO.

Characterizing the Morphology of Nanocomposites

Mechanical features are said to be one of the most crucial components since they relate to the homogeneity of various morphologies, domain sizes, and forms to define the degree of dispersion of interactions between the two stages [22]. In general, polyblend with rich phase domain size, improved

interface contact area, and higher interfacial bond is produced by an operative compatibilizer. SEM was used to observe the microstructural characterization of TPE/nZnO nanocomposites. The morphological evidence of broken surfaces in the TPE/U3nZnO, TPE/C3nZnO, and TPE/C5nZnO nanocomposite samples is shown in Figure 3(a–c). Figure 3(a) shows that there was poor compatibility between TPE and nZnO, as evidenced by the random dispersion of nZnO particles in TPE/U3nZnO and the presence of multiple large agglomerates on the fracture surface with particle sizes larger than 1 μm. The TPE had irregularly distributed nZnO particles, several of which were agglomerated and were carried into bigger cavities surrounding the agglomerates. The hydrophilic ZnO nanoparticles' agglomeration into TPE makes sense. Higher agglomeration results when a certain amount of hydroxyl groups create hydrogen bonds with TPE and nanoparticles. Since there are no functional polymers in the TPE/nZnO nanocomposite due to the dispersion of larger nanoparticles, the component bonding appears to be rather weak, and the surfaces are individually wetted. This makes possible the later-discussed reduced tensile characteristics of the nanocomposites. We discovered that these were made up of several fundamental particles after realizing this aggregation. SEM pictures of the TPE/C3nZnO and TPE/C5nZnO nanocomposites are shown in Figure 3(b–c), respectively. The morphology is altered by TPE/3nZnO or TPE/5nZnO presence. In comparison to TPE/C5nZnO nanocomposite, the fractured surface morphology of TPE/C3nZnO nanocomposite was more homogeneous and finer, and its mean particle size was smaller. The influence of SEBSMA strengthened the interfacial bond between TPE and nZnO. When the nZnO surface was coated with SEBSMA, it distributed randomly in TPE, avoiding agglomerations and filling voids. Additionally, there was a higher cohesive force and more homogenous incorporation of C3nZnO in the TPE matrix. nZnO has been covered with SEBSMA, which has also enhanced nZnO and TPE matrix compatibility. The large-scale plastic distortion of the TPE can be persuaded by these acceptable holes and nanoparticles, strengthening the fracture.

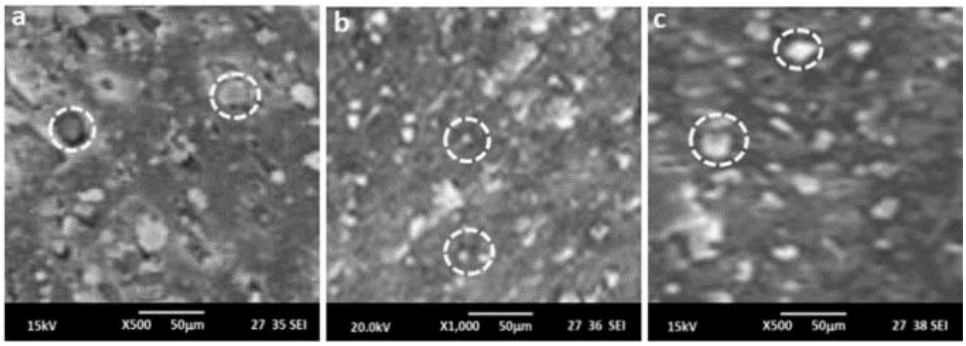

Figure 3. TPE/nZnO nanocomposites (w/w%) as seen in SEM images. (a) TPE/U3nZnO, (b) TPE/C3nZnO, and (c) TPE/C5nZnO.

The Nanocomposites' Thermal Characteristics

Table 1 shows the DSC results for virgin TPE and its nanocomposites (TPE/nZnO). The results showed that the ZnO nanoparticle addition to TPE might have an impact on the PTMG segment's melting temperature (T_m). The T_m of the PTMG segment rises from 88.3°C of the matrix to 99.5°C of nanocomposites at 1 wt% of ZnO nanoparticles. The T_m of the PTMG segment in the nanocomposite was 5.1°C lower than that of virgin TPE at 5 wt% of ZnO nanoparticles.

The T_m of the PBT segment of the TPE/nZnO nanocomposite is only marginally enhanced relative to the TPE matrix, but it has a similar lowering tendency with nanoparticle loading, in contrast to the substantially affected T_m of the PTMG segment in nanocomposites. The greatest increase in T_m (PBT) is 4.5°C, and it happens at 1% wt%age of ZnO nanoparticles. The T_m of PBT and PTMG segments should grow in nanocomposites to facilitate the chemical bonding of ZnO nanoparticles with the matrix. On the other hand, TPE containing ZnO nanoparticles can lower the composition's wt%age of PTMG and PBT segments. This could be the result of T_m (PTMG) and T_m (PBT) in nanocomposites

decreasing as the number of nanoparticles increases. Furthermore, it was thought that most of the chemical interactions between the ZnO nanoparticles and matrix occurred on the nanoparticles that survived in the PBT/PTMG amorphous phase, where the PTMG segment is quite large. Because of this, the PTMG part experiences a more noticeable increasing effect on T_m than the PBT section. A different outcome of the chemical bonding between ZnO nanoparticles and matrix was a decrease in the chemical regularity of the macromolecular chain, which was indicated by a decrease in the crystal enthalpy (ΔH_c) shown in Table 1 and a subsequent crystallization of the hard PBT section in nanocomposites. Table 1 transfers the PBT section's crystalline temperature (T_c) to a higher temperature within the nanocomposite. The nuclear effect of ZnO nanoparticles should be taken into consideration due to the rise in T_c of the PBT section in nanocomposites. Table 1 provides a list of every datum that was acquired throughout DSC examinations.

Table 1. TPE and TPE/nZnO nanocomposites' thermal characteristics.

NCs (wt%)		T_m (°C)	T_c (°C)	ΔH_c (J/g)	T_{onset} (°C) (TGA)
	PTMG Block	**PBT Block**	**PBT Block**		
V. TPE	88.3	176.8	134.6	25.2	393.5
U3nZn	99.5	181.3	136.5	22.1	395.6
C3nZnO	96.2	178.6	137.3	21.9	402.4
C5nZnO	94.4	177.5	136.9	21.4	397.5

Note: NCs: Nanocomposites; V: Vargin; U3nZnO: TPE/U3nZnO; C3nZnO: TPE/C3nZnO.

Important evidence regarding the temperature stabilities of the nanocomposites is provided by the TGA investigation. One important property for which the shape of the nanocomposite was crucial was thermal stability [23]. Figure 4 shows the TGA thermograms of TPE/nZnO nanocomposites and virgin TPE. In the temperature range of 349–470°C, it may be assumed that all the samples show a one-step degradation process. Virgin TPE and its nanocomposites lose less than 0.02% of their weight at 349°C, and the moisture content of the matrix is significantly reduced. At an acute pace, key breakdown associated with the decrease of the matrix backbone in virgin TPE begins at approximately 349°C. The thermal stability of a material is shown by the average temperature degradation temperature (T_{onset}) of TPE, which is 393.5°C. An increase in the thermal degradation temperature of the nanocomposite with a higher nanoparticle loading indicates that the addition of ZnO nanoparticles enhances the matrix's thermal stability. At 3 wt% of nanoparticles, the largest increase in thermal stability is 8.9°C.

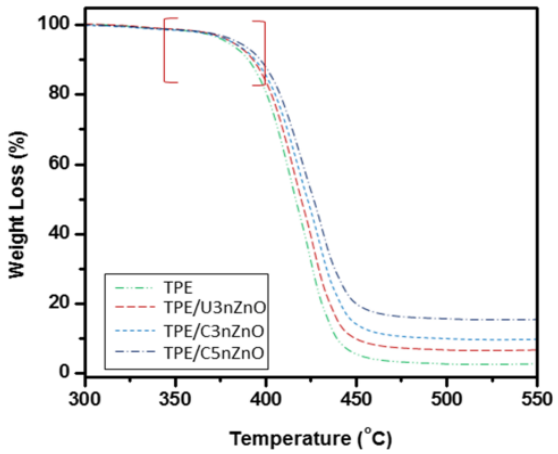

Figure 4. TGA curves for nanocomposites made of TPE and TPE/nZnO.

Mechanical Characteristics of TPE/SEBS Composites

The mechanical properties of the polymer matrix are advanced by metal oxide nanoparticles [24]. The variation of TPE, TPE/UnZnO nanocomposites with nZnO levels ranging from 0 to 5 wt%, and

TPE/CnZnO nanocomposites with the same contents as nZnO is shown in Figure 5. It is shown that raising the nZnO content to 3 wt% enhanced both the yield strength and the tensile strength (for TPE/U3nZnO nanocomposites, the yield strength increased by 20% and the tensile strength by 25%, and for TPE/C3nZnO nanocomposites, the yield strength increased by 43% and the tensile strength increased by 38% compared to TPE, respectively) before declining by 5 wt%. By combining the increased characteristics with the nanofiller spread, one may identify increased yield and tensile strength. Because there is a high stress transfer from TPE to nZnO, adding nZnO particles to the TPE increases the yield and tensile strength of the matrix at 3 wt% nZnO. The relatively low-stress transmission impact of nZnO particles minimized an improvement in yield and tensile strength at 5 wt% of nZnO particles. In this instance, the agglomerated nanoparticles are readily separated from the TPE, and the yield and tensile strength are not eventually lowered by any portion of the external load. Zaman et al. provided support for these results [25]. SEBSMA prompted the modification of TPE/nZnO nanocomposites to enhance the interfacial bonding between nZnO particles and TPE. Compared to TPE/nZnO nanocomposites, the interfacial bonding between the filler and matrix has been noticeably stronger when SEBSMA is added to TPE/nZnO blends. At 3 wt% of nZnO content, the maximum yield and tensile strength of the TPE/C3nZnO nanocomposite were 23.9 and 25.3 MPa, respectively, and were approximately 43% and 38% higher than those of the TPE matrix. Better distribution from the compatibilizer and improved solid-state adhesion, which can transmit more stress from the matrix to the dispersion phase, are two ways in which the strengthened compatibilized system can be manifested. The ethylene butylene mid-block of SEBS has been grafted with MA functional groups. After that, it transforms from SEBSMA molecular chains into TPE and forms bonds with metal oxides. As a result, it is possible to create uniform, finely distributed structures.

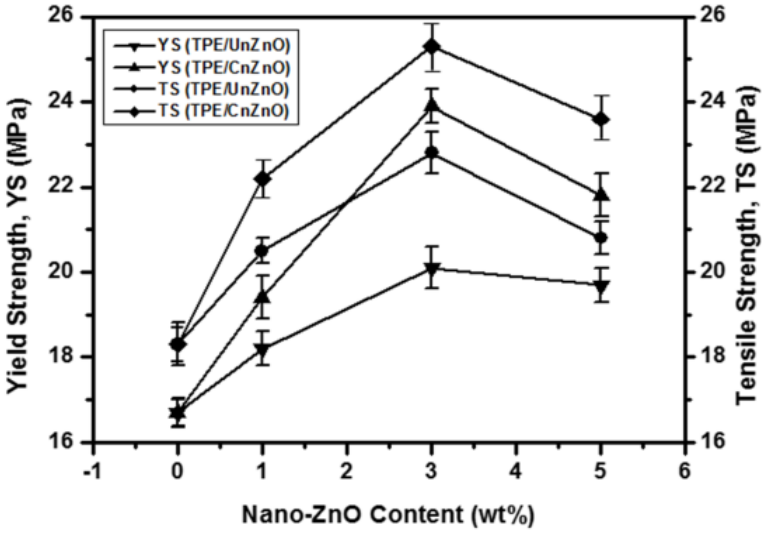

Figure 5. Yield strength and tensile strength of TPE/nZnO nanocomposites.

Tensile modulus and elongation of TPE/nZnO nanocomposites are shown to vary with nZnO content in Figure 6. Tensile modulus increased steadily while elongation at break decreased steadily with nZnO addition. Modulus growth provides an effective stress transfer from TPE to nZnO particles, but the elongation decreased with nZnO addition indicates interference or deformability of TPE by nZnO, which was brought about by physical interaction and mechanical restraint of the TPE. The maximum TM (303.6 MPa) of TPE/UnZnO nanocomposite was obtained at 5 wt% of nZnO content. At this point, the TM value of the nanocomposite was approximately 48% higher than that of the TPE matrix. The TPE/CnZnO nanocomposite rose more noticeably than the TPE/UnZnO nanocomposite, based on the modulus variant trajectory. The reduction in elongation at break was observed in the presence of nZnO, suggesting that nZnO was involved in influencing the TPE's deformability or mobility. TPE and the presence of mechanical restraint interacted physically to achieve this intervention. This indicates that the TPE nanocomposite becomes stiffer as the

concentration of nZnO rises because the elongation at break decreases periodically. On the other hand, compared to uncoated nZnO nanocomposite, SEBSMA coated nZnO nanocomposites displayed reduced elongation at break. These findings support morphological observations and show a substantial interaction between TPE and nZnO. Since TPE has improved nZnO expansion and the facial stress bridge between TPE and nZnO, it has a greater influence on nZnO than TPE.

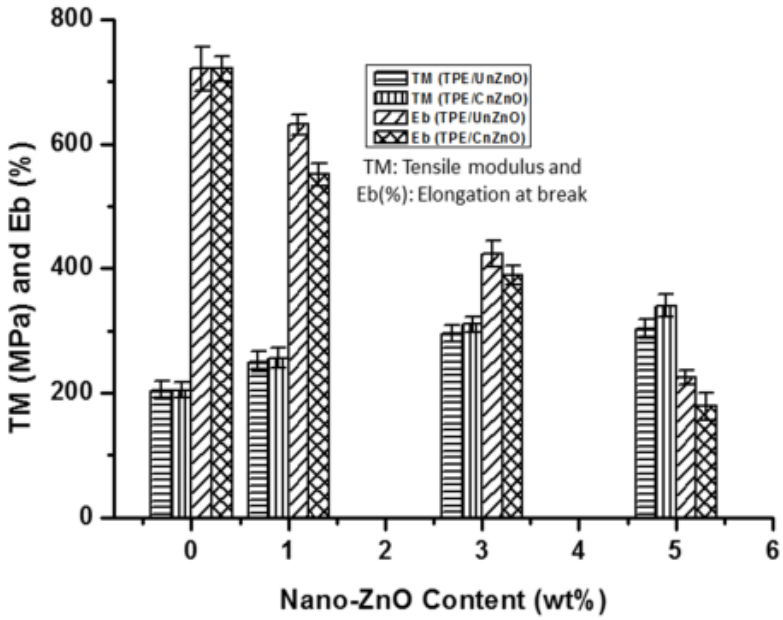

Figure 6. The TPE/nZnO nanocomposites' tensile and elongation at break.

Electrical Characteristics

With nZnO concentration, the resistivity and dielectric constant of coated and uncoated TPE/nZnO nanocomposites were investigated at a fixed frequency of 10 kHz. The dielectric constant of the coated and uncoated TPE/nZnO nanocomposite varies with nZnO content, as shown in Figure 7(a). When the amount of nZnO in nanocomposites increases, the dielectric constant rises almost linearly. When the nZnO concentration is investigated at roughly 5 wt%, there is also no abrupt increase in the dielectric constant in the nZnO content, which is also referred to as the percolation phenomena, for these nanocomposites. This is most likely caused by nZnO's low-dielectric characteristic. When it comes to other polymers or high dielectric fillers (such carbon nanotubes) in nanocomposites, when percolation thresholds or concentrations exist, this behavior is much different [26]. Agglomeration of filler particles at percolation thresholds causes cluster structures to emerge in most polymer/filler composites. For filler luster to occur with relatively modest filler content, such a structure is appropriate. It is evident from this that the fillers in TPE/nZnO nanocomposites are distributed throughout the matrix as separate particles rather than clumping together as low-nZnO particle clusters. The dielectric behavior of the composite is also significantly influenced by the dispersion of fillers in the polymer matrix. In polyolefins like polypropylene or polythene, SEBSMA typically works well as a compatibilizer to distribute fillers [27]. Accordingly, adding SEBSMA to the TPE/nZnO nanocomposite will enhance the dispersion of nZnO nanoparticles inside the TPE matrix, preventing the agglomeration and formation of a pathway network of nZnO particles.

Resistivity to the nZnO content of TPE/nZnO nanocomposites is displayed in Figure 7(b). TPE that is virgin has a resistivity of ~ 2.6×10^{11} Ω-m. When TPE/nZnO nanocomposites are added, their resistivity starts to drop up to 2 wt%, and when the nZnO concentration is increased, it lowers practically continuously after that. The resistivity of nanocomposites drops to ~ 0.24×10^{11} Ω-m in 5 wt% nZnO. For virgin TPE, this translates to almost 91 decreases. Percolation theory provides an explanation of resistivity in this regard.

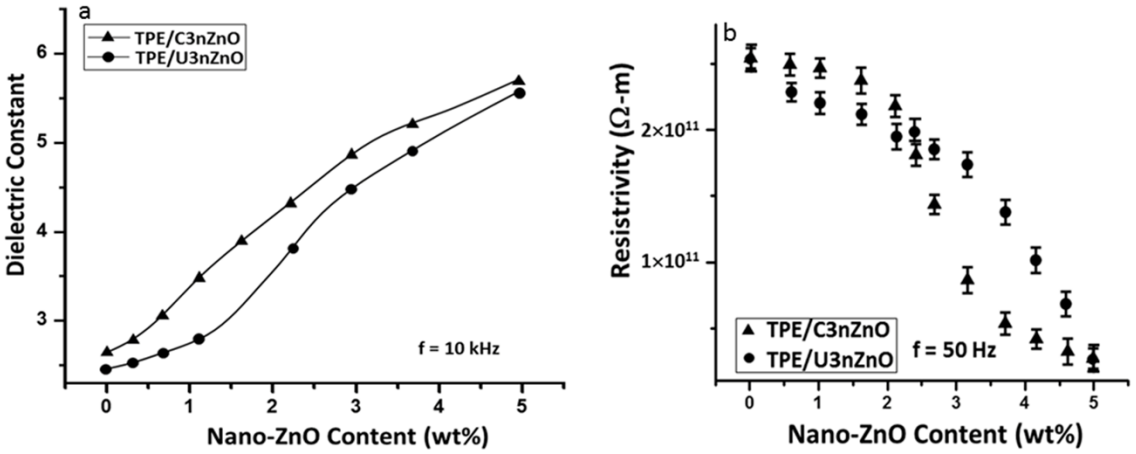

Figure 7. TPE/nZnO nanocomposites: (a) dielectric constant and (b) resistivity as a function of nano-ZnO content (wt%).

CONCLUSION

PBT-PTMG based TPE/nZnO nanocomposite has been used to prepare a melt mixing procedure that will be followed by the hot compression molding technique. This study looked at how surface-modified nZnO particles affected the TPE matrix nanocomposites' mechanical, morphological, thermal, and electrical characteristics. Polymers that have nZnO added to them have increased in strength, stiffness, and thermal stability, but their elongation at break has significantly decreased. Therefore, at 3 wt% filler concentration, morphological investigations have demonstrated improved interaction between the SEBSMA coated filler and the matrix. The tiny and consistent crystal size distribution of SEBSMA coated-nZnO has improved the thermal characteristics of the composites. It has been studied how the size of the ZnO particles in the coating affects the resistivity and dielectric constant. The results demonstrate that when nZnO concentration increases, the dielectric constant of nanocomposites increases almost linearly. The resistivity of the nanocomposites drastically reduces when the nZnO content rises above 2.5 wt%. Percolation theory can be used to explain this characteristic. It is concluded that the mechanical, thermal, and electrical properties improved with the addition of fillers.

REFERENCES

1. Bae J, Lee S, et al. Polyester-based thermoplastic elastomer/MWNT composites: rheological, thermal, and electrical properties. Fiber Polym. 2013;14:729–735.
2. Zhan J, Ma L, et al. Mechanical, thermal, and flame-retardant behaviors of thermoplastic polyether–ester elastomer composites with polyphenylene oxide and aluminum hypophosphite. Poly Plast Tech Engin. 2017;56:1096–1107.
3. Gregory GL, Sulley GS, et al. Triblock polyester thermoplastic elastomers with semi-aromatic polymer end blocks by ring-opening copolymerization. Chem Sci. 2020;11(25):6567–6581.
4. Parcheta P, Głowińska E, et al. Effect of bio-based components on the chemical structure, thermal stability and mechanical properties of green thermoplastic polyurethane elastomers. Europe Poly J. 2020;123:109422.
5. Jiang J, Tang Q, et al. Structure and morphology of thermoplastic polyamide elastomer based on long-chain polyamide 1212 and renewable poly (trimethylene glycol). Indust Engin Chem Res. 2020;59:17502–17512.
6. Zanchin G, Leone G. Polyolefin thermoplastic elastomers from polymerization catalysis: advantages, pitfalls and future challenges. Progr Poly Sci. 2020;113;101342.
7. Jiang R, Chen Y, et al. Preparation and characterization of high melt strength thermoplastic polyester elastomer with different topological structure using a two-step functional group reaction. Polymer. 2019;179:121628.
8. Yao C, Yang G. Crystallization, and morphology of poly (trimethylene terephthalate)/poly

(ethylene oxide terephthalate) segmented block copolymers. Polymer. 2010;51:1516–1523.
9. Ryou JH, Ha CS, et al. Miscibility of poly (vinyl methyl ether) and poly (styrene-co-2-vinylnaphthalene) blends by FT-IR spectroscopy and Tg measurements. J Poly Sci Part A Poly Chem. 1993;31:325–333.
10. Džunuzović E, Jeremić K, et al. In situ radical polymerization of methyl methacrylate in a solution of surface modified TiO2 and nanoparticles. Europe Poly J. 2007;43:3719–3726.
11. Convertino A, Leo G, et al. TiO2 colloidal nanocrystals functionalization of PMMA: a tailoring of optical properties and chemical adsorption. Sens Actuat B Chem. 2007;126:138–143.
12. Lu S-R, Zhang H-L, et al. Studies on the properties of a new hybrid materials containing chain-extended urea and SiO2–TiO2 particles. Polymer. 2005;46:10484–10492.
13. Mishra PK, Mishra H, et al. Zinc oxide nanoparticles: a promising nanomaterial for biomedical applications. Drug Discov Today. 2017;22:1825–1834.
14. Kim S, Lee SY, et al. Doxorubicin-wrapped zinc oxide nanoclusters for the therapy of colorectal adenocarcinoma. Nanomaterials. 2017;7:354.
15. Zhang Z-Y, Xiong H-M. Photoluminescent ZnO nanoparticles and their biological applications. Materials. 2015;8:3101–3127.
16. Tjong S, Bao S. Fracture toughness of high density polyethylene/SEBS-g-MA/montmorillonite nanocomposites. Compos Sci Tech. 2007;67:314–323.
17. Wang Z, Lu Y, et al. Preparation of nano-zinc oxide/EPDM composites with both good thermal conductivity and mechanical properties. J Appl Poly Sci. 2011;119:1144–1155.
18. Ray SS, Okamoto M. Polymer/layered silicate nanocomposites: a review from preparation to processing. Progr Poly Sci. 2003;28:1539–1641.
19. Altan M, Yildirim H. Mechanical and antibacterial properties of injection molded polypropylene/TiO2 nano-composites: effects of surface modification. J Mat Sci Tech. 2012;28:686–692.
20. Li J, Hong R, et al. Effects of ZnO nanoparticles on the mechanical and antibacterial properties of polyurethane coatings. Progr Org Coat. 2009;64:504–509.
21. American Society for Testing and Materials. D638−14. Standard Test Method for Tensile Properties of Plastics. 2014;17.
22. Ghazy O, Freisinger B, et al. Tuning the size and morphology of P3HT/PCBM composite nanoparticles: towards optimized water-processable organic solar cells. Nanoscale. 2020;12:22798–22807.
23. Kilburn D, Dlubek G, et al. Free volume in poly (n-alkyl methacrylate)s from positron lifetime and PVT experiments and its relation to the structural relaxation. Polymer. 2006;47:7774–7785.
24. Rahman M, Hoque MA, et al. Study on the mechanical, electrical and optical properties of metal-oxide nanoparticles dispersed unsaturated polyester resin nanocomposites. Result Phys. 2019;13:102264.
25. Zaman HU, Hun PD, et al. Effect of surface-modified nanoparticles on the mechanical properties and crystallization behavior of PP/CaCO3 nanocomposites. J Thermoplast Comp Mat. 2013;26:1057–1070.
26. Sung JH, Kim HS, et al. Nanofibrous membranes prepared by multiwalled carbon nanotube/poly (methyl methacrylate) composites. Macromolecules. 2004;37:9899–9902.
27. Tjong S, Meng Y. Impact-modified polypropylene/vermiculite nanocomposites. J Poly Sci Part B Poly Phys. 2003;41:2332–2341.

